IMAGING AND CALIBRATION IN THE PRESENCE OF DIRECTION DEPENDENT EFFECTS

S. Bhatnagar[(1)], T.J. Cornwell[(2)], and K. Golap[1]

[(1)] *National Radio Astronomy Observatory, Socorro, NM, USA*
[(2)] *Australia Telescope National Facility, Sydney, Australia*
E-Mails: sbhatnag@nrao.edu, kgolap@nrao.edu, Tim.Cornwell@csiro.au

Abstract

Direction dependent effects can be classified as known/measured effects (which need not be solved for) and unknown effects which need to be solved for. The effects of non co-planar baselines, asymmetric primary beams, primary beam squint, etc. are examples of the first kind, while effects of antenna pointing offsets, ionospheric/atmospheric effects and spectral index effects of the sky are examples of the unknown direction dependent effects. Correction of all these type of effects is vital to achieve the advertised sensitivities and imaging dynamic ranges of the upcoming and planned new generation aperture synthesis radio telescopes. Fast application of such effects in iterative imaging and deconvolution algorithms and solving for the unknown effects are the two major challenges. This paper presents our work on techniques for the fast application of such effects as well as solve for some of the unknown effects like the antenna pointing offsets.

1 Introduction

Measurement Equation for an interferometer can be compactly written using the HBS notation [1] as

$$V_{ij}^{Obs} = \mathsf{J}_{ij} \int \mathsf{J}_{ij}^{Sky}(\boldsymbol{S}) I(\boldsymbol{S}) e^{\iota \boldsymbol{S}.\boldsymbol{B}_{ij}} d\boldsymbol{S} \tag{1}$$

where V_{ij}^{Obs} and V_{ij}^{M} are the observed and model visibility Stokes vectors, J_{ij} is the Muller Matrix composed of multiplicative antenna based gains and $\mathsf{J}_{ij}^{Sky}(\boldsymbol{S})$ is the Muller Matrix of direction dependent gains as a function of direction $\boldsymbol{S}$, and I is the image. When J_{ij}^{Sky} is unity, the above equation reduces to $V_{ij}^{Obs} = \mathsf{J}_{ij} V_{ij}^{M}$. The effects of J_{ij} can be removed prior to imaging by multiplying this equation by $\mathsf{J}_{ij}^{\mathrm{T}}$ and using the corrected visibility for making the image. The effects of J^{Sky} however cannot be similarly removed since it is an image plane effect and hence must be corrected for during imaging. Direction dependent effects which are antenna independent (and hence same for all baselines) can be removed by dividing the image by J^{Sky}. Un-squinted antenna power pattern is one such example. For El-Az mounted antennas with a squint in the power patterns of the two orthogonal polarizations, image plane polarization properties not only change across the field of view but also rotate on the sky as a function of parallactic angle (PA). As long as the squint is same across the antennas, such errors can still be corrected, to a large extend, by correcting individual snapshot dirty images for each polarization (or dirty images in some PA increment) and combining them to make the final dirty image which is then used as the update direction in the deconvolution iterations as:

$$\boldsymbol{I}_k^d = \int \mathsf{J}_k^{Sky^{-1}}(\psi) \mathcal{FT}\left[\mathsf{J_{ij}}^{-1} \boldsymbol{V}_{ij}^{Obs}(\psi)\right]_k d\psi \tag{2}$$

where ψ is the parallactic angle and the above equation is evaluated in appropriate increments of ψ. Since removing the effects of J_{ij} is not an issue, for the rest of this paper, J_{ij} will be assumed to be unity.

Antenna pointing errors make J^{Sky} different for each baseline making it expensive to evaluate the inversion of Eq. 1 for each image pixel. For high dynamic range imaging and when images are represented as a collection of components (as is done in Asp-Clean [2] or MS-Clean deconvolution), it may be possible to efficiently evaluate Eq. 1. Work on that will the subject of another future paper. Here we describe techniques to efficiently correct for primary beams including polarization squint and pointing errors as part of the iterations of the image deconvolution algorithms.

2 Direction dependent error correction

Eq. 1 can be re-phrased to express the predicted model visibilities as

$$\boldsymbol{V}_P^{M'} = \mathsf{E}_P \mathsf{A} \boldsymbol{I}_P^M \tag{3}$$

where the subscript P represents a polarization product, A is the Measurement Matrix, $\mathsf{E}_P = \mathsf{A}\mathsf{J}_P^{Sky}\mathsf{A}^{\mathrm{T}}$ (the data domain representation of J^{Sky}), and $\boldsymbol{I}^M$ is the model image. When J^{Sky} is same for all antennas, approximating the Hessian as a diagonal matrix, the update direction can be computed as

$$\Delta \boldsymbol{I}^{\boldsymbol{D}} = -\Re\left[\mathsf{J}^{\mathsf{Sky}\dagger}\mathsf{J}^{\mathsf{Sky}}\right]^{-1}\Re\left[\mathsf{J}^{Sky\dagger}\boldsymbol{I}^{\boldsymbol{R}}\right] \tag{4}$$

where J^{Sky} is computed in appropriate increment of the Parallactic Angle (PA).

However when J^{Sky} is antenna dependent (different for each baseline in the visibility domain), direction dependent effects cannot be reduced to multiplicative effects in the image domain. In such cases, applying the correction in the image domain becomes impractical (requires data from each baseline to be inverted for each image pixel). Such effects must then be incorporated by evaluating Eq. 3 for visibility prediction in the major cycle of deconvolution algorithms.

The algorithm to incorporate direction dependent effects during imaging is motivated by the w-projection algorithm [3]. The transform is accurately computed in one direction (image to data) and an approximate update direction is computed and the model image is iteratively improved as $\boldsymbol{I}_i^M = \boldsymbol{I}_{i-1}^M + \alpha \max\left[\Delta \boldsymbol{I}_{\mathrm{i}}^{\mathrm{D}}\right]$ $(0 < \alpha < 1)$. Errors due to the approximation are iteratively corrected in the accurate prediction of the model visibilities to achieve convergence.

2.1 The forward and inverse transforms

When direction dependent errors are present, the predicted model visibilities are given by Eq. 3. Typically, since the measured visibilities are not on a regular grid, model visibilities are predicted from $\mathsf{A}\boldsymbol{I}^M$ as:

$$\boldsymbol{V}^{M'}(u,v,w) = \left(\mathsf{G}\left[\mathsf{A}\boldsymbol{I}^M\right]^g\right)(u,v,w) \tag{5}$$

where G is the operator for the convolution by the Gridding Convolution Function (GCF) and superscript g indicates data on a regular grid. Direction dependent effects redistribute the energy in the visibility plane and the focusing operation must reflect this via G, which in general is complex valued. For visibility prediction then, Eq. 3 can be straightforwardly used - provided E has appropriate aliasing properties and can be efficiently evaluated for each baseline. Transform in this forward direction will be accurate and this is all that is required for the update direction computation in Pointing SelfCal algorithm to solve for E given a reasonably accurate model image [4].

Since the inverse transform may not strictly exist, a pseudo-inverse transform $[\mathsf{AE}_p]^{\mathrm{T}}$ can be used to transform from the data to the image domain. The image however will have an extra multiplication by J^{Sky}. An approximate update direction can be computed with correct units by dividing the image formed using the pseudo-inverse operator by an average J^{Sky} over all antennas.

3 Results

We used the above approach for direction dependent correction to develop algorithms to solve for antenna based pointing offsets [4] as well as correct for the effect of pointing offsets during image deconvolution. The pointing offsets are solved by minimizing $\chi^2 = \boldsymbol{V}^{\mathbf{R}^{\mathrm{T}}}\boldsymbol{V}^{\mathbf{R}}$ where $\boldsymbol{V}^{\mathrm{R}} = \boldsymbol{V}^{\mathrm{M}} - \boldsymbol{V}^{\mathrm{Obs}}$. $\boldsymbol{V}^{\mathrm{M}}$ is evaluated using Eq. 5 and G is parameterized by the antenna pointing offsets. The primary beams for the two orthogonal polarizations for the VLA antennas are offset by a fixed amount from the pointing direction ($\sim 6\%$ of the FWHM of the primary beam). This causes spurious features in Stokes-V and the effect increases with the distance from the pointing center.

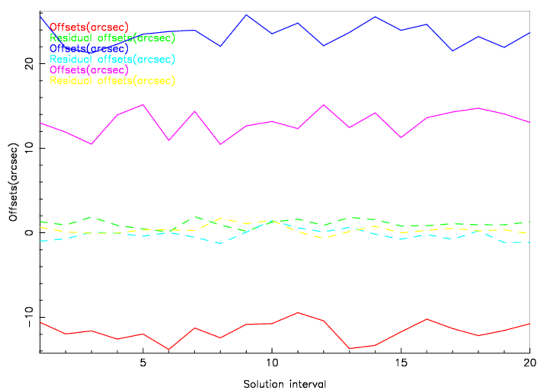

Figure 1: Typical antenna pointing offsets used in the simulation (x-axis spans $4hr$).

The data was simulated for 1400MHz for the VLA C-array configuration. The sky was simulated using sources from the NVSS survey. The time varying antenna pointing offsets, with the mean value for each antenna randomly distributed between $\pm 20''$ and RMS pointing offsets of $5''$ was used to simulate typical pointing errors for VLA antennas. The pointing offsets used in the simulation are shown as continuous lines in Fig. 1. The model image was then used to iteratively solve for the pointing offsets. The residual pointing offsets after the convergence was achieved, shown as dashed lines in Fig. 1, has a RMS of $\sim 1''$.

Fig. 2 shows the Stokes-I deconvolved image before and after correction for pointing and squint offsets. Errors in the image on the left are at the level of $\sim 15\mu$Jy. The solved pointing offsets, along with the know VLA polarization squint error were then used in the forward and inverse transform during the iterative deconvolution to correct for pointing and squint error during imaging. Fig. 3 shows the Stoke-V images before and

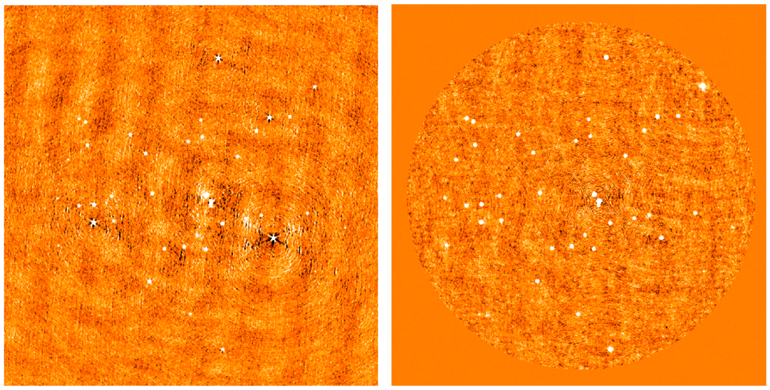

Figure 2: Stokes-I images before (left) and after (right) pointing/squint correction.

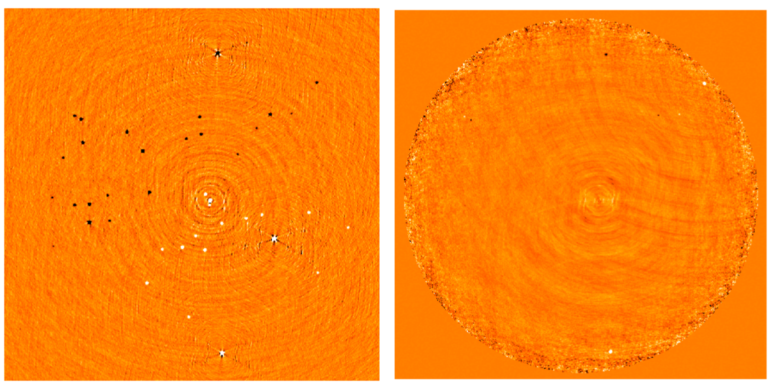

Figure 3: Stokes-V images before (left) and after (right) pointing/squint correction.

after applying such correction. The errors in the image on the right are dominated by the squint error. The peak and RMS noise in the images are 2mJy and $\sim 15\mu$Jy/beam and 20μJy and $\sim 1\mu$Jy/beam respectively. The peak errors in the image on the right are due the assumptions of a uniform, unobstructed aperture illumination.

References

[1] J. P. Hamaker, J. D. Bregman, and R. J. Sault. Understanding radio polarimetry. i. mathematical foundations. *A&AS*, 117:137–147, May 1996.

[2] S. Bhatnagar and T. J. Cornwell. Scale sensitive deconvolution of interferometric images. I. Adaptive Scale Pixel (Asp) decomposition. *A&A*, 426:747–754, November 2004.

[3] T. J. Cornwell, K. Golap, and S. Bhatnagar. W-projection: A new algorithm for non-coplanar baselines. Technical report, EVLA Memo 67, Dec. 2003.

[4] S. Bhatnagar, T. J. Cornwell, and K. Golap. Solving for the antenna based pointing errors. Technical report, EVLA Memo 84, Aug. 2004.